

# Reengineering Rate-Limiting, Millisecond Enzyme Motions by Introduction of an Unnatural Amino Acid

Eric D. Watt,<sup>†</sup> Ivan Rivalta,<sup>†</sup> Sean K. Whittier,<sup>‡</sup> Victor S. Batista,<sup>†</sup> and J. Patrick Loria<sup>†‡\*</sup>

<sup>†</sup>Department of Chemistry and <sup>‡</sup>Department of Molecular Biophysics and Biochemistry, Yale University, New Haven, Connecticut

**ABSTRACT** Rate-limiting millisecond motions in wild-type (WT) Ribonuclease A (RNase A) are modulated by histidine 48. Here, we incorporate an unnatural amino acid, thia-methylimidazole, at this site (H48C-4MI) to investigate the effects of a single residue on protein motions over multiple timescales and on enzyme catalytic turnover. Molecular dynamics simulations reveal that H48C-4MI retains some crucial WT-like hydrogen bonding interactions but the extent of protein-wide correlated motions in the nanosecond regime is decreased relative to WT. NMR Carr-Purcell-Meiboom-Gill relaxation dispersion experiments demonstrate that millisecond conformational motions in H48C-4MI are present over a similar pH range compared to WT. Furthermore, incorporation of this nonnatural amino acid allows retention of WT-like catalytic activity over the full pH range. These studies demonstrate that the complexity of the protein energy landscape during the catalytic cycle can be maintained using unnatural amino acids, which may prove useful in enzyme design efforts.

## INTRODUCTION

Optimal enzyme activity requires that the protein possess the ability to undergo fluctuations between conformations. The important role of conformational flexibility in protein function (1) is underscored by efforts to incorporate elements of flexibility into the protein design process (2–5) to enhance or modulate the desired function. The amplitudes and mechanisms of these motions are often complex and occur over an enormous timescale range (6). The bond making/breaking steps in an enzyme-catalyzed reaction occur on the timescale of tens of femtoseconds (fs). Yet, the overall rates of catalytic reactions occur in tens to hundreds of milliseconds (ms), a range of 12 orders of magnitude. Thus, the overwhelming majority of events that occur during the course of enzyme-catalyzed reactions occur before and after the reaction transition state (7–13). The energy landscape on which enzyme reactions take place is extremely complex in which slower, barrier-crossing millisecond motions are often responsible for preparing the substrate and the enzyme active site for reaction and for facilitating the release of products once the reaction is complete, whereas faster thermal motions can contribute to the thermodynamics of ligand binding (14). The enormity of the timescales involved makes investigation of enzyme function a daunting task. Nonetheless, obtaining deeper insight into enzyme function and the role these motions play, requires that this issue be addressed. Motional events that occur with such a large diversity in timescale can be investigated, in part, through a combination of molecular dynamics (MD) simulations to obtain atomistic insight into thermal motions that are faster than a few nanoseconds, and NMR relaxation dispersion experiments that probe

$\mu$ s–ms motions. Here, we combine these two methods along with the introduction of an unnatural amino acid at a critical enzyme residue to address the robustness of enzyme function and motions to perturbations, which are not accessible by standard site-directed mutagenesis.

These issues are investigated in the enzyme ribonuclease A (RNase A) in which millisecond motions have been demonstrated to be of functional importance and where motions optimize the enzyme conformation at distinct stages along the enzymatic reaction coordinate (15,16). RNase A possesses the innate ability to presample the relevant ligand-bound conformations even in the absence of ligand (15). Studies on RNase A since the mid-1960s have implicated a histidine residue in the functional motion in this enzyme on the basis of temperature jump and NMR pH titration experiments (17,18). More recent NMR relaxation dispersion experiments have identified and characterized the role in which hydrogen bonding associated with histidine 48 (H48) plays in these important protein motions (19,20). In RNase A motions that are distant (20 Å) from the enzyme's active site are propagated, via H48, between loop 1 (residues 14–24) to  $\beta$ -strands 1 and 4, which contain active-site residues T45 and D83, respectively. These residues provide important pyrimidine-specificity interactions at the active site and ultimately modulate the enzyme's rate-limiting step, which is a conformational change associated with product release. In contrast, the chemistry step in RNase A is rapid and  $k_{\text{cat}}/K_M$  is limited by substrate association with the enzyme and approaches the diffusion limit (21). Replacement of hydrogen bonding interactions around H48 with deuterium resulted in a normal kinetic solvent isotope effect on enzyme motions from 1800 s<sup>-1</sup> to 800 s<sup>-1</sup> and similar reduction in the measured  $k_{\text{cat}}$  value (20). Furthermore, studies have demonstrated the sensitivity of the region surrounding H48 to mutagenesis, which in all

Submitted March 28, 2011, and accepted for publication May 19, 2011.

\*Correspondence: patrick.loria@yale.edu

Editor: Josh Wand.

© 2011 by the Biophysical Society  
0006-3495/11/07/0411/10 \$2.00

doi: 10.1016/j.bpj.2011.05.039



and  $^{15}\text{N}$  dimensions using the program Sparky. One-dimensional slices were then individually and globally fit to the McConnell equations using the program LineShapeKin (<http://lineshapekin.net/>). Comparison of fits using Akaike's information criterion indicated that global fitting was preferred in each case by a factor of at least 700.

## Modeling and MD simulations

The computational structural models for WT, H48C, and H48C-4MI enzymes are based on the crystal structure of the phosphate-free RNase A refined at 1.26 Å (Protein Data Bank code 7RSA) (32). All water molecules in the crystal structure were kept in the computational studies. All MD simulations were based on the AMBER-ff99SB (33) force field, as implemented in the NAMD2 software package (34). The generalized Amber force field (35) has been used for the nonstandard residue present in the thia-methylimidazole enzyme (H48C-4MI). The partial charges for this nonstandard residue were derived by using the RESP method (36) based on Hartree-Fock (HF)/6-31G\* calculations performed with the GAUSSIAN 09 package (37).

Production MD runs have been performed after the following preequilibration procedure: hydrogen atoms and explicit TIP3P water (38) solvent molecules (~8890) were added using AmberTools (version 1.4) and subsequently optimized, constraining the rest of the atoms at the crystal structure positions. A short optimization of the side chain of residue 48 has been performed only in the case of H48C and H48C-4MI mutants. The optimized solvated structures were then slowly heated to 298 K by performing MD simulations (100 ps) in the canonical NVT ensemble using Langevin dynamics. Harmonic constraints have been applied to the protein heavy atoms, with force constants set to 1 kcal/mol/Å<sup>2</sup>. During this heating procedure different parts of the system were gradually unconstrained until all atoms were set free. Fully unconstrained MD simulations were run for 4.9 ns, for a total preequilibration simulations of 5 ns.

Upon system preequilibration, 20 ns MD simulations were performed in the NPT ensemble at 298 K and 1 atm using the Langevin piston. All simulations were performed using periodic boundary conditions. Electrostatics were treated with the particle mesh Ewald method (39) and van der Waals interactions were calculated using a switching distance of 10 Å and a cutoff of 12 Å. A multiple time stepping algorithm (40) was used, where bonded, short-range nonbonded, and long-range electrostatic interactions were evaluated at every one, two, and four time steps, respectively, using a time step of integration set to 1 fs.

The  $\text{C}\alpha$ - $\text{C}\alpha$  covariance matrix is computed according to the Pearson correlation coefficient:

$$r[x_i, x_j] = \langle x_i \cdot x_j \rangle / \left( \langle x_i^2 \rangle \langle x_j^2 \rangle \right)^{1/2},$$

where  $x_i$  is the nuclear coordinates of atom  $i$  relative to the ensemble average value, where  $\langle \rangle$  denotes the ensemble average over the entire MD simulation. This is an established method typically used for quantifying correlated motion in proteins from MD simulations (41).

## RESULTS AND DISCUSSION

Site-specific chemical modifications to introduce unnatural chemical functionalities that are not available in the standard genetic code have previously been used to study enzyme mechanisms and motions. Early applications include proteases in which S195 of chymotrypsin was converted to dehydroalanine (42) and the active-site hydroxyl from subtilisin was replaced with a thiol (43,44). This early work exploited the special reactivity of these active site groups to achieve the desired modification. Coupling of chemical modification

with site-directed mutagenesis allowed modulation of the chemical and physical properties at nearly any desired position. In the late 1980's, Smith et al. (45) and Kirsch and co-workers (46,47) exploited thiol reactivity to selectively incorporate aminoethylcysteine residues into ribulose biphosphate carboxylase/oxygenase and aspartate aminotransferase, respectively, enabling this modified amino acid to carry out the normal lysine mediated enzymatic reaction. Furthermore, unnatural amino acids have been incorporated to introduce a spectroscopically active probe to interrogate protein structure and dynamics by Raman, infrared, electron paramagnetic resonance, and NMR spectroscopies (48–54). These spectroscopic studies have shed light on the functional role of protein dynamics but are limited in scope, due to the single probe being located at an isolated site in the protein structure. Characterization of the effects of an unnatural amino acid substitution on the dynamics of the entire enzyme would enable detailed insight into the energy landscape on which these motions occur.

In RNase A, histidine 48 was mutated to cysteine by standard site-directed mutagenesis protocols. Subsequently, we expressed and purified  $^{15}\text{N}$ -labeled H48C RNase A and reacted the resulting free thiol, introduced at position 48, with 4-chloromethylimidazole (4-CMI) (26) (Scheme 1). For WT RNase A, there are no free thiols in the enzyme, thus mutation of H48 to cysteine and subsequent chemical derivatization with 4-CMI results in incorporation of a single, 4-methyl imidazole (4-MI) group, which was verified by 5,5'-dithiobis-(2-nitrobenzoic acid) analysis (27). This single-site introduction of an unnatural amino acid results in replacement of histidine with an analog containing sulfur and an additional methylene group and is therefore two chemical bonds longer than histidine (Scheme 1 and Fig. 1 a). The larger side chain of 4-MI results in an increase in volume of this residue to 133.2 Å<sup>3</sup> from that of a histidine side chain, which is 98.2 Å<sup>3</sup>. In addition, it is expected that the thioether linkage will alter the  $\text{pK}_a$  of the methylimidazole side chain to some extent. Fig. 1 shows a comparison of  $^1\text{H}$ - $^{15}\text{N}$  NMR spectra for uniformly  $^{15}\text{N}$ -labeled WT, H48C, and H48C-4MI enzymes. The mean composite  $^1\text{H}$  and  $^{15}\text{N}$  chemical shift difference from WT is  $0.11 \pm 0.07$  ppm for H48C-4MI, suggesting that chemical modification of C48 results in little perturbation of the RNase A structure. These chemical shift changes are localized to the site of mutation (Fig. S1 in the Supporting Material). The largest differences ( $+1.5\sigma$ ) from WT for H48C-4MI are located at the end of loop 1 (Y25),  $\beta_1$  (K41 and T45),  $\alpha_3$  (L51, D53, V54, and Q55),  $\beta_4$  (D83, C84, and E86), and  $\beta_5$  (T100). Small chemical shift changes from WT values were also observed in studies on the H48C and H48A RNases A (20). In addition, the H48C-4MI resonance peaks are mostly positioned between H48C and WT suggesting that the modification of C48 by 4-MI results in an enzyme structure that more closely resembles the WT than the cysteine mutant from which it is derived. This similarity

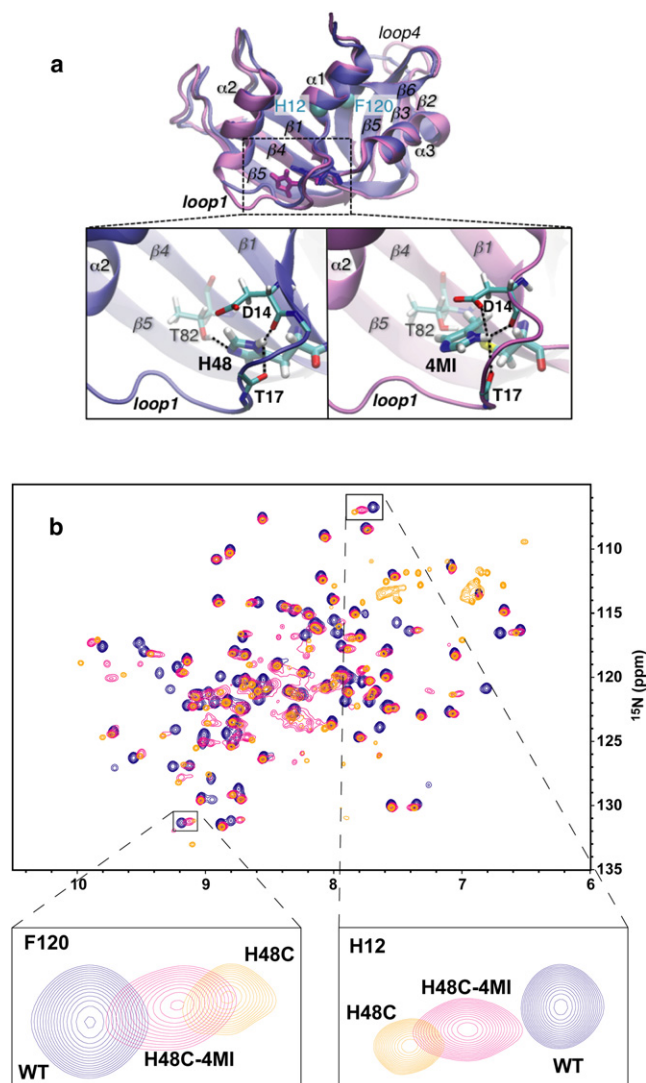


FIGURE 1 Comparison of WT, H48C, and H48C-4MI. (a) Average backbone structure WT and H48C-4MI over a 20 ns MD simulation and expansion showing H-bond interactions with loop 1 and  $\beta$ -strand 4 that are common to H48 and H48C-4MI. Secondary structures and relevant residues are labeled. Part (b) shows an overlay of  $^1\text{H}$ ,  $^{15}\text{N}$  HSQC spectra for WT, H48C, and H48C-4MI. Peaks are labeled to indicate the RNase A variant. The expanded region shows a close up view of F120 and H12 showing the proximity of the H48C-4MI peak to WT, relative to the H48C residues. Contour levels were adjusted to account for different [RNase A].

with WT extends to sites of protein conformational motions as described below.

### Millisecond motions in H48C-4MI

Conformational exchange motions can be quantitatively characterized by Carr-Purcell-Meiboom-Gill (CPMG) NMR relaxation dispersion experiments. In these experiments, the transverse relaxation rate constant ( $R_2$ ) is measured as a function of the CPMG pulse spacing ( $\tau_{\text{cp}}$ ) in a spin-echo experiment. In many cases, conformational motion manifests as dispersion in the measured  $R_2$  value as a function of  $\tau_{\text{cp}}$  in

which the kinetic ( $k_{\text{ex}}$ ), thermodynamic (populations, ( $p_{a/b}$ )), and structural (chemical shift differences ( $\Delta\omega$ )) details of the motion can be determined (55). In the fast limit in which  $k_{\text{ex}} > \Delta\omega$ ,  $k_{\text{ex}}$  and the exchange contribution to the NMR resonance ( $R_{\text{ex}} = p_a p_b \Delta\omega^2 / k_{\text{ex}}$ ) can be determined. In other cases, conformational motion is evident in the form of elevated  $R_2$  values compared to rigid sites within the protein but shows no variation with  $\tau_{\text{cp}}$ , usually indicating that motion is faster than the interval between the CPMG  $180^\circ$  pulses. To investigate motions in RNase A, we performed these experiments on  $^{15}\text{N}$ ,  $^2\text{H}$ -WT,  $^{15}\text{N}$ ,  $^1\text{H}$ -H48C, and  $^{15}\text{N}$ ,  $^1\text{H}$ -H48C-4MI at different solution pH values. Exchange broadening of several of the residues in loop 1 in the H48C-4MI enzyme (pH 6.4) precludes quantitation of motional parameters and suggests that motions are on the intermediate exchange timescale in H48C-4MI, unlike what is observed in H48C or H48A (Fig. S2 and Fig. S3), in which these sites are rigid. In loop 1, T17 (Fig. S3) shows elevated  $R_2$  values but no dispersion in H48C-4MI indicating that this residue retains its flexibility but its motion has likely moved to a somewhat faster timescale. A similar effect is observed for T45 in  $\beta 1$  and C84 in  $\beta 4$  (Fig. S2 and Fig. S3, Table S1). Conversion of H48C to H48C-4MI restores ms motions at pH = 6.4 as shown by  $R_{\text{ex}}$  contributions to  $R_2$  for V43 that are  $>0$  ( $3.2 \pm 1.8 \text{ s}^{-1}$ ). In addition, in  $\beta 1$ , three residues (F46, V47, and MI48) are unassigned in H48C-4MI at pH 6.4 and 7.0, due to being exchange broadened. Nonetheless, the H48C-4MI enzyme shows conformational exchange at similar sites to WT enzyme, which is not the case for the H48C enzyme (Fig. S3, Fig. S4, Fig. S5 and Table S1). Overall, relaxation rates could be quantitated for 109, 106, 78, and 98 residues, respectively, for WT (pH = 6.4 and 7.0) and H48C-4MI (6.4 and 7.0).

One aspect of the involvement of H48 in WT RNase A motions is that above and below the pK range for histidine, no evidence for motions is present in the region surrounding H48 such as in loop1,  $\beta 1$ , and  $\beta 4$ . The flat dispersion curves that are characteristic of a lack of ms motions, at these pH values, are shown in Fig. S6. In contrast, at pH = 6.4 and 7.0 the functionally important motions in WT are evident (Figs. 2 and S6). For WT residues S22, V43, and C84 the CPMG dispersion curves at pH = 6.4 and 7.0 show the upward curvature that is characteristic of ms motions (Fig. 2 and Fig. S6). These results indicate that the rate-limiting motions in WT RNase A occur within a small pH window. Motions for residues that are not part of the loop1,  $\beta 1$ , and  $\beta 4$  regions, such as N71, are not affected significantly by the changes in solution pH (Fig. 2, and Fig. S3 and Fig. S6) (20). These pH insensitive regions are also not affected by mutagenesis to H48, surrounding sites, or loop 1 indicating that they are distinct from the rate-limiting motions in loop1,  $\beta 1$ , and  $\beta 4$  (22,56).

Mutation to H48C, like previous mutations in this region, results in the elimination of ms motions in loop1,  $\beta 1$ , and  $\beta 4$

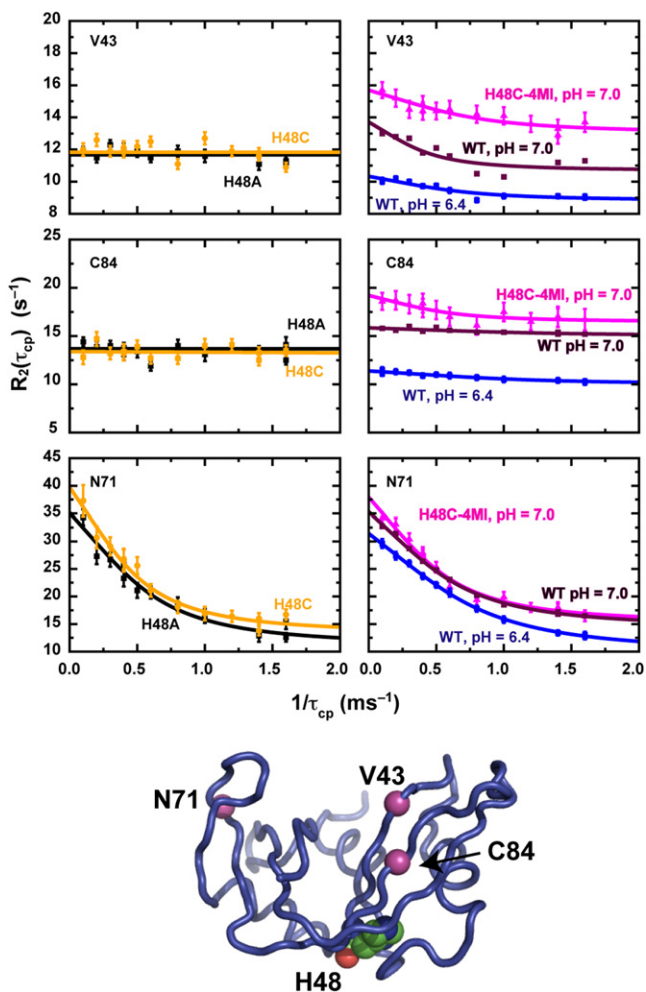


FIGURE 2 Millisecond motions in H48C-4MI. Dispersion curves for V43, C84, and N71 are displayed. On the left are dispersion curves for  $^1\text{H}, ^{15}\text{N}$ -H48A pH = 6.4 and  $^1\text{H}, ^{15}\text{N}$ -H48C, pH = 7.0. The right panel shows CPMG dispersion curves  $^2\text{H}, ^{15}\text{N}$ -WT, pH = 6.4 and  $^1\text{H}, ^{15}\text{N}$ -pH = 7.0 and  $^1\text{H}, ^{15}\text{N}$ -H48C-4MI pH = 7.0. Labels identifying the appropriate enzyme are placed closest to the relevant dispersion curve. The data are fit with the fast-limit CPMG dispersion equation. The ribbon structure of RNase A shows the location of these residues as single spheres. The side chain of thia-imidazole is shown as a sphere representation.

(Fig. 2). For many residues in H48C-4MI at pH = 6.4, evidence for ms motions at sites similar to WT comes from elevated  $R_2$  values and observation of exchange broadened residues (Fig. S2, Fig. S3, Fig. S4, Fig. S5, Table S1). For WT RNase A, NMR data have established that the functionally important global conformational motions in WT RNase A cluster in loop 1,  $\beta_1$ , and  $\beta_4$  and move with an exchange rate constant,  $k_{\text{ex}} = 1800 \text{ s}^{-1}$  at 298 K and pH = 6.4 and 7.0 (15,16,19,20,56). Likewise, at pH 7.0 for H48C-4MI upward sloping dispersion curves are observed for V43 and C84 on  $\beta_1$  and  $\beta_4$ , respectively (Fig. 2), which are indicative of conformational exchange motion. Global fits of the fast-limit form of the CPMG dispersion equation to these two residues give a  $k_{\text{ex}} = 1650 \pm 450 \text{ s}^{-1}$ , which is

nearly identical to WT values (Fig. 2). Motions in loop 4 as evidenced by residue N71, indicate that it retains WT-like motions and is not affected by the thia-imidazole substitution at residue 48 (Figs. 2 and S3) (16,20,22). Other residues in  $\beta_1$  and  $\beta_4$  remain sufficiently exchanged broadened at pH = 7.0 such that quantitation of these motions are not possible for these residues (Fig. S4). These data indicate that placing a larger imidazole group at position 48 is compatible within the WT enzyme structure and can restore ms motions that are similar to WT RNase A.

### MD simulations of H48C-4MI

Molecular motions on timescales of several ns provide atomistic information on the ensemble of populated conformers that are accessible to the macromolecule. To investigate the effects of an unnatural amino acid substitution on ns timescale motions, we have modeled the effects of the 4-MI incorporation in a 20 ns MD simulation of H48C, H48C-4MI, and WT at 298 K, with emphasis on the analysis of H-bonding interactions with loop 1 and  $\beta_4$  that are common to H48 and H48C-4MI. Fig. 1a shows a comparison of representative snapshot configurations for WT and H48C-4MI. The region around loop 1 (backbone root mean-square deviation 1.87 Å) is highlighted, including hydrogen bonds with side chains in loop 1 (D14 and T17) and  $\beta_4$  (T82). When comparing the relative stability of these fundamental interactions, we find that H48 in WT RNase A maintains an H-bond with the side chain of T82 as well as H-bonding interactions with loop 1 over the entire simulation time. Due to thermal fluctuations, however, the H-bond that is made with loop 1 is formed alternately with D14 for 75% of the time and with T17 for the rest of the simulation. Analogously, the longer and more flexible side chain of H48C-4MI stabilizes H-bonding interactions with T82 and D14 for 60% and 30% of the simulation time, respectively. The unprotonated nitrogen of the imidazole ring of H48C-4MI is alternately forming H-bonds with the polar side chains of T82 or Q101, or with the N-H group of the A20 backbone. In addition, the imidazole NH group of H48C-4MI forms H-bonds with the side chains of T82 or Y25, or with D14. Overall, the main H-bond interactions of H48 with T82 and D14 in WT are maintained in the H48C-MI enzyme, indicating that the most relevant interactions with loop 1 and  $\beta$ -strand 4 are present with the 4-MI single-site chemical modification of H48C (Fig. S7, Fig. S8, Fig. S9). However, the 4-MI group is more promiscuous over the 20 ns simulation, forming transient hydrogen bonding interactions with a number of other residues. These additional interactions made by the methylimidazole side chain are likely due to the additional rotational degrees of freedom relative to that of histidine.

We additionally analyzed the  $C\alpha$ - $C\alpha$  covariance matrix over the entire 20 ns simulation for each enzyme. Shown in Fig. 3 are the results of this analysis for WT, H48C-4MI,

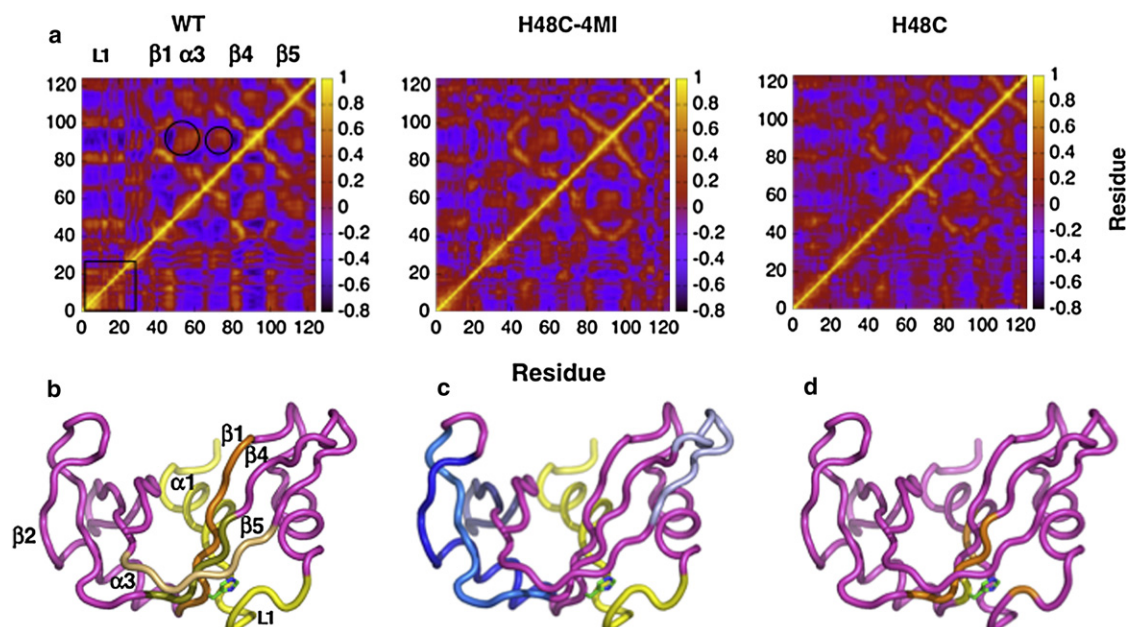


FIGURE 3 Covariance analysis of ns motions in RNase A. In *a*, motional correlations are shown for WT, H48C-4MI, and H48C from a 20 ns MD simulation. Panels *b–d* show results for WT mapped onto a cartoon ribbon of RNase A. Positive correlations (*b*) between residues 1–22 and  $\beta 1$ ,  $\beta 4$ , and  $\beta 5$  are shown. Panel *c* shows anticorrelations between residues 1–22 and  $\beta 2$ ,  $\alpha 3$ , and  $\beta 5$ . Panel *d* shows positive correlations between H48 (*stick rendering*) and loop 1,  $\beta 1$ , and  $\beta 4$ .

and H48C. Qualitatively, it is clear that the extent of motional correlation in H48C-4MI more closely resembles that of WT than does H48C. In addition to correlations between loop 1 and the rest of the enzyme, correlations are decreased in the  $\alpha 3$  and  $\beta 3$  regions and loop residues 85–95 (*circled areas* in Fig. 3). The correlations in secondary structure in WT are shown in Fig. 3 *b–d*. In Fig. 3 *b* positive correlations with  $\alpha 1$ /loop 1 with  $\beta 1$ , 4, and 5 are indicated. In Fig. 3 *d*, correlations between H48 and parts of  $\beta 4$  and loop 1 are shown. Whereas, in Fig. 3 *c*, anti-correlated regions between  $\alpha 1$ /loop 1 and  $\beta 2$ ,  $\alpha 3$ , and the N-terminal portion of  $\beta 4$  are indicated in shades of blue. Modification of C48 with methylimidazole does not fully restore WT-like ns motions or the high degree of correlated motions throughout the protein, yet the H48C-4MI is more WT-like in its fast motion behavior than is the H48C protein.

#### 4-MI restores ligand-binding interactions

Having addressed the motional properties of H48C-4MI, we next investigated the impact of this unnatural amino acid on RNase A function. Upon interaction with the product analog (3'-CMP), the NMR resonance signals in WT RNase A show linear progression until saturation is reached, which is characteristic of a two-state bimolecular binding reaction. The resulting apparent  $K_d$  for 3'-CMP for WT is 500  $\mu\text{M}$  at pH 7.0 (57,58). Fig. 4 shows the chemical shift change for D121, Q11, H12, and E86 as a function of [3'-CMP] for H48C-4MI and H48C at pH = 7.0. The apparent 3'-CMP

dissociation constants for these four residues, individually, are within 3% of each other and therefore all four were fit to obtain a single, apparent  $K_d = 300 \pm 9 \mu\text{M}$  for H48C-4MI at pH = 7.0 (Fig. 4 *a*). In H48C, the affinity for 3'-CMP is weaker ( $K_d = 610 \pm 32 \mu\text{M}$ , Fig. 4 *b*) than in H48C-4MI enzyme. The introduction of 4-methylimidazole results in slightly tighter binding for H48C-4MI compared to WT RNase A.

The kinetics of interaction between WT RNase A and the reaction product determine the overall rate of catalytic turnover in this enzyme (21). Furthermore, the ms motions in RNase A have been demonstrated to be coupled to the release of product. The rate constant of 3'-CMP dissociation from RNase A can be determined by NMR lineshape analysis. In  $^1\text{H}$ - $^{15}\text{N}$ -WT RNase A under conditions in which ms motions are present,  $k_{\text{off}}$  for 3'-CMP determined by lineshape analysis is  $1700 \pm 500 \text{ s}^{-1}$  (16,22,56). In Fig. 5, the data used to determine  $k_{\text{off}}$  for  $^1\text{H}$ - $^{15}\text{N}$ -H48C-4MI and  $^1\text{H}$ - $^{15}\text{N}$ -H48C are shown. For H48C-4MI,  $k_{\text{off}}$  for 3'-CMP is  $1920 \pm 750 \text{ s}^{-1}$  and is similar to  $k_{\text{ex}}$  measured for motions in this chemically modified enzyme. This  $k_{\text{off}}$  value is also similar to that obtained for WT enzyme. In contrast, the data for H48C are at the upper limit for accurate measurements. The minimal line broadening at intermediate 3'-CMP titration points indicates fast dissociation. The uncertainty in fitted  $k_{\text{off}}$  for H48C is high,  $k_{\text{off}} = 10,500 \pm 2700 \text{ s}^{-1}$  and we estimate that  $k_{\text{off}}$  in the H48C mutant is at least  $6000 \text{ s}^{-1}$  and thus ligand dissociates much faster from this enzyme than WT or H48C-MI, which have similar  $k_{\text{off}}$  values.

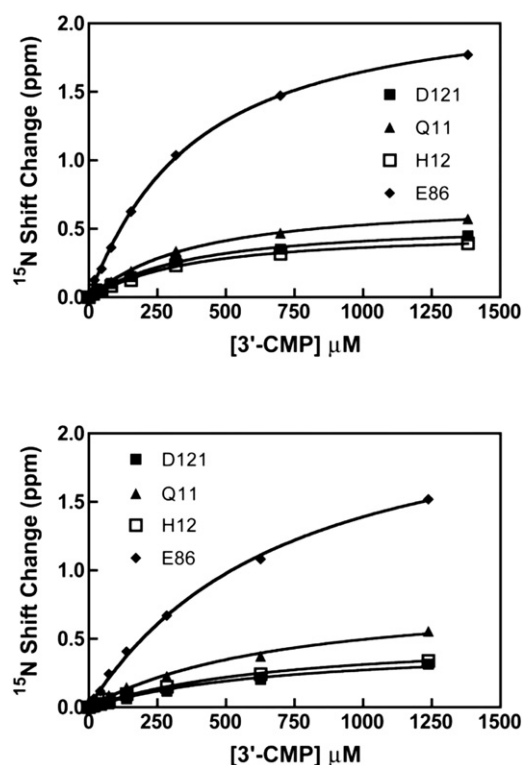


FIGURE 4 Binding of  $^{3'}\text{-CMP}$  to RNase A. (Top) H48C-4MI (bottom) H48C.  $^1\text{H}$ ,  $^{15}\text{N}$  chemical shift changes for four residues are plotted versus the concentration of  $^{3'}\text{-CMP}$  at pH = 7.0, 298 K. All data are fit with a single global one-site binding model.

### H48C-4MI is catalytically active

The  $k_{\text{cat}}/K_{\text{M}}$  values for WT RNase A with a fluorescent substrate (28) (6-carboxyfluorescein- $\sim$ dArU(dA) $_2$ -6-carboxytetramethylrhodamine) indicate that its cleavage is limited by the rate of enzyme encounter with substrate. For WT, at 0.1 M NaCl and pH = 7.0  $k_{\text{cat}}/K_{\text{M}}$  for this substrate is  $3.6 \times 10^7 \text{ M}^{-1} \text{ s}^{-1}$  (59). We investigated the effect of solution pH on  $k_{\text{cat}}/K_{\text{M}}$  for WT and H48C-4MI (Fig. 6). Fitting Eq. 1. to the data gave  $-\log$  of the acidic ( $\text{pK}_{\text{a}}$ ) and basic ( $\text{pK}_{\text{b}}$ ) equilibrium values of  $4.1 \pm 0.1$  ( $4.7 \pm 0.1$ ) and  $6.8 \pm 0.1$  ( $6.6 \pm 0.1$ ) for WT (H48C-4MI), respectively. The WT  $\text{pK}$  values obtained here are consistent with prior work on this enzyme (21). The instability of the substrate at acidic conditions precludes measurements at lower pH values. Thus, the  $\text{pK}_{\text{a}}$  value determined from the fits are highly dependent on the data point at pH = 4.3. Therefore, we estimate the uncertainty in the  $\text{pK}_{\text{a}}$  is slightly higher than the fitted error of 0.1 pH units. These data show similar catalytic activities over a similar pH range for WT and H48C-4MI.

## CONCLUSIONS

Enzyme motions are essential for their function. Understanding how the structure and flexibility of the protein

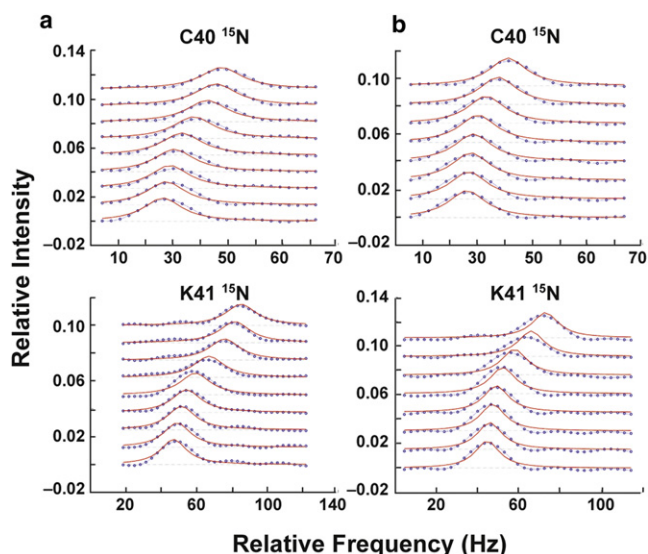


FIGURE 5 Kinetics of product,  $^{3'}\text{-CMP}$  interactions with RNase A. In *a*, global lineshape fitting to C40 and K41 in H48C-4MI. Panel (*b*) shows lineshape results for the same residues in H48C. All lineshape experiments were performed on protonated enzyme.

shapes the energy landscape over the course of the catalytic cycle is crucial for drug and protein design as well as protein engineering efforts. The complexity of this problem necessitates that multiple and unique experimental methods be used. In this work, we introduce an unnatural amino acid at a single site in uniformly  $^{15}\text{N}$ -labeled RNase A and subsequently characterize the effects of this amino acid substitution on protein motions, function, and structure.

The similarity between the  $^1\text{H}$ - $^{15}\text{N}$  HSQC spectra for WT, H48C-4MI, and H48C indicate that the structure of RNase A is not significantly altered by modification at position 48. Thus, the native fold of RNase A is robust and tolerant to single-site perturbations. This conclusion is further supported by the similarity in computationally optimized models of WT, H48C, and H48C-4MI (Fig. 1 *a*). In addition, almost all NMR resonances in H48C-4MI are positioned

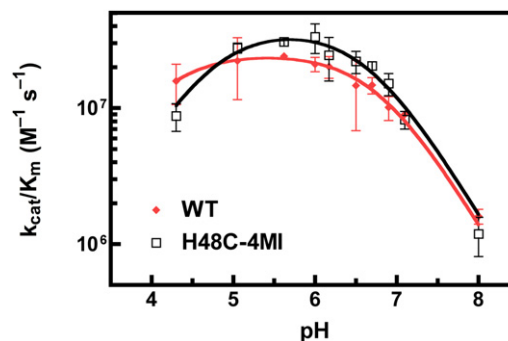


FIGURE 6 Catalytic activity in RNase A. pH dependence of  $k_{\text{cat}}/K_{\text{M}}$  for WT (diamonds) and H48C-4MI (squares) are shown. Equation 1 was fit to the data to determine  $\text{pK}$  values. Error bars are derived from multiple measurements.

closer to the WT peak than the corresponding resonance in H48C suggesting that the 4-MI modification shifts the average solution structure to more closely resemble that of WT enzyme than does the H48C variant.

Perhaps the most interesting feature of the H48C-4MI RNase A is the similarity in pH range in which ms motions are present compared to WT. The cysteinyl methylimidazole group must be able to satisfy the main requirement that H48 does for facilitation of motion for residues in loop 1,  $\beta 1$ , and  $\beta 4$ . In addition, this chemical modification does not alter distant flexible regions of RNase A that have been shown to be uncoupled from residue 48. Thus, the 4-MI residue does not introduce nonnatural motions elsewhere in the enzyme. The kinetics of motion in H48C-4MI are the same, at pH = 7.0, as those in WT at pH = 6.4 and pH = 7.0. In addition, these motions occur at similar sites in the two enzymes suggesting similar motional mechanisms. Moreover, the onset of millisecond motions requires the covalent linkage to the imidazole moiety because the H48G mutant in the presence of >50 mM imidazole shows no conformational exchange motions (Fig. S10), indicating that ms motions cannot be rescued by addition of endogenous imidazole.

The amplitude of the relaxation dispersion curves,  $R_{\text{ex}} = p_a p_b \Delta\omega^2 / k_{\text{ex}}$ , reflects both contributions from the equilibrium populations and chemical shift differences due to the conformational motions, which in the fast conformational exchange limit cannot be resolved into individual terms. Nonetheless, the ratio of WT and H48C-4MI dispersion curve amplitudes is the same for V43 and C84 and is equal to  $0.56 \pm 0.30$  and  $0.51 \pm 0.16$ , respectively. Yet for N71 there is no effect with  $R_{\text{ex}}^{\text{WT}} / R_{\text{ex}}^{\text{H48C-4MI}} = 0.95 \pm 0.11$ . The unnatural amino acid at position 48 likely affects the populations of the two conformations and not  $\Delta\omega$  because the  $^1\text{H}$  of V43 and C84 are far from residue 48, 15.3 Å, and 9.0 Å, respectively. In addition, the isotropic chemical shifts of V43 and C84 are very close to their WT positions. Therefore effects, if any, on  $\Delta\omega$  should be rather small for these two residues. Thus, the identical increase in  $R_{\text{ex}}$  for V43 and C84 suggests that it is the equilibrium populations ( $p_a p_b$ ) that are primarily affected. This change in populations reflects about a 2 kcal/mol change in the relative differences in energy levels between the two conformations. However, the similar  $k_{\text{ex}}$  for WT and H48C-4MI suggests the barrier height between the two conformations remains the same. This conclusion will require further testing for validation.

The function of H48C-4MI is not dramatically altered relative to WT RNase A. The methylimidazole group of H48C-4MI fully restores WT binding affinity of the product analog 3'-CMP. This suggests that the H-bonding interactions made by the imidazole side chain are functionally important for ligand binding and these interactions are not satisfied by the thiol of cysteine but are sufficiently reestablished by 4-MI modification. Moreover, the pH rate data indicate that 4-methylimidazole at position 48 does not alter

the ionization constants of the active site residues to an extent that it alters the catalytic activity of RNase A or its substrate association rate. The model for Michaelis complex formation in RNase A involves a diffusion-limited encounter complex followed by rearrangement to form the RNase A/substrate complex (21). Incorporation of an unnatural amino acid in RNase A does not alter this aspect of the RNase A energy landscape. This may turn out to be a clinically useful property of RNase A in which its cancer-killing ability requires catalytic activity but also the ability to evade Ribonuclease inhibitor (RI) (60). If binding to RI relies in part on the ms motions in RNase A, incorporation of unnatural amino acids may promote lower affinity interactions with RI and yet maintain high levels of catalytic activity.

In conclusion, we have exploited the versatility afforded by insertion of an unnatural amino acid into RNase A by chemical modification of a unique cysteine residue. The enzyme containing thia-methylimidazole at residue 48 possesses motions in similar regions, on similar timescales, and over a similar pH range as WT enzyme. These motions are selectively incorporated into one region of the enzyme without affecting existing motions in a separate region. These results demonstrate that conformational exchange motions may be amenable to rational engineering provided that details of motions in the WT enzyme are known in advance, such that the appropriate modification can be introduced. Furthermore, these studies indicate that chemical modification can be a route to introduce subtle alterations at amino acid sites for the study of protein motions. This should pave the way for in-depth study of the chemical and physical properties of dynamically important residues.

## SUPPORTING MATERIAL

A table and 10 figures are available at [http://www.biophysj.org/biophysj/supplemental/S0006-3495\(11\)00609-6](http://www.biophysj.org/biophysj/supplemental/S0006-3495(11)00609-6).

We thank Professors Jeff Hoch and Mark Maciejewski (University of Connecticut) for the generous use of their Varian 600 MHz NMR equipped with a cryogenically cooled probe. We thank Roger Cole and Gennady Khirich for NMR data obtained at pH = 4.5, 7.0, and 7.5.

J.P.L. acknowledges support from the National Science Foundation (NSF) MCB-0744161. E.D.W. and S.K.W. were recipients of a National Institutes of Health (NIH) biophysical training grant (5T32GM008283). V.S.B. acknowledges support for Dr. Rivalta from NIH 1R01-GM-084267-01 and GM-043278 and supercomputing time from the National Energy Research Scientific Computing Center (NERSC).

## REFERENCES

1. Karplus, M., and J. Kuriyan. 2005. Molecular dynamics and protein function. *Proc. Natl. Acad. Sci. USA.* 102:6679–6685.
2. Desjarlais, J. R., and T. M. Handel. 1999. Side-chain and backbone flexibility in protein core design. *J. Mol. Biol.* 290:305–318.
3. Harbury, P. B., J. J. Plecs, ..., P. S. Kim. 1998. High-resolution protein design with backbone freedom. *Science.* 282:1462–1467.
4. Nauli, S., B. Kuhlman, and D. Baker. 2001. Computer-based redesign of a protein folding pathway. *Nat. Struct. Biol.* 8:602–605.

5. Su, A., and S. L. Mayo. 1997. Coupling backbone flexibility and amino acid sequence selection in protein design. *Protein Sci.* 6:1701–1707.
6. Frauenfelder, H., G. Chen, ..., R. D. Young. 2009. A unified model of protein dynamics. *Proc. Natl. Acad. Sci. USA.* 106:5129–5134.
7. Hammes, G. G., R. W. Porter, and G. R. Stark. 1971. Relaxation spectra of aspartate transcarbamylase. Interaction of the catalytic subunit with carbamyl phosphate, succinate, and L-malate. *Biochemistry.* 10:1046–1050.
8. Hedstrom, L., L. Szilagyi, and W. J. Rutter. 1992. Converting trypsin to chymotrypsin: the role of surface loops. *Science.* 255:1249–1253.
9. Sampson, N. S., and J. R. Knowles. 1992. Segmental motion in catalysis: investigation of a hydrogen bond critical for loop closure in the reaction of triosephosphate isomerase. *Biochemistry.* 31:8488–8494.
10. Alber, T., W. A. Gilbert, ..., G. A. Petsko. 1983. The role of mobility in the substrate binding and catalytic machinery of enzymes. *Ciba Found. Symp.* 93:4–24.
11. Erman, J. E., and G. G. Hammes. 1966. Relaxation spectra of ribonuclease. IV. The interaction of ribonuclease with cytidine 2':3'-cyclic phosphate. *J. Am. Chem. Soc.* 88:5607–5614.
12. Erman, J. E., and G. G. Hammes. 1966. Relaxation spectra of ribonuclease. V. The interaction of ribonuclease with cytidyl-3':5'-cytidine. *J. Am. Chem. Soc.* 88:5614–5617.
13. Jayaraman, V., K. R. Rodgers, ..., T. G. Spiro. 1995. Hemoglobin allostery: resonance Raman spectroscopy of kinetic intermediates. *Science.* 269:1843–1848.
14. Cooper, A., and D. T. F. Dryden. 1984. Allostery without conformational change. A plausible model. *Eur. Biophys. J.* 11:103–109.
15. Beach, H., R. Cole, ..., J. P. Loria. 2005. Conservation of mus-ms enzyme motions in the apo- and substrate-mimicked state. *J. Am. Chem. Soc.* 127:9167–9176.
16. Kovrigina, E. L., and J. P. Loria. 2006. Enzyme dynamics along the reaction coordinate: critical role of a conserved residue. *Biochemistry.* 45:2636–2647.
17. French, T. C., and G. G. Hammes. 1965. Relaxation spectra of ribonuclease. II. Isomerization of ribonuclease at neutral pH values. *J. Am. Chem. Soc.* 87:4669–4673.
18. Markley, J. L. 1975. Correlation proton magnetic resonance studies at 250 MHz of bovine pancreatic ribonuclease. II. pH and inhibitor-induced conformational transitions affecting histidine-48 and one tyrosine residue of ribonuclease A. *Biochemistry.* 14:554–561.
19. Cole, R., and J. P. Loria. 2002. Evidence for flexibility in the function of ribonuclease A. *Biochemistry.* 41:6072–6081.
20. Watt, E. D., H. Shimada, ..., J. P. Loria. 2007. The mechanism of rate-limiting motions in enzyme function. *Proc. Natl. Acad. Sci. USA.* 104:11981–11986.
21. Park, C., and R. T. Raines. 2003. Catalysis by ribonuclease A is limited by the rate of substrate association. *Biochemistry.* 42:3509–3518.
22. Doucet, N., E. D. Watt, and J. P. Loria. 2009. The flexibility of a distant loop modulates active site motion and product release in ribonuclease A. *Biochemistry.* 48:7160–7168.
23. Butterwick, J. A., and A. G. Palmer, 3rd. 2006. An inserted Gly residue fine tunes dynamics between mesophilic and thermophilic ribonucleases H. *Protein Sci.* 15:2697–2707.
24. Chakravorty, D. K., and S. Hammes-Schiffer. 2010. Impact of mutation on proton transfer reactions in ketosteroid isomerase: insights from molecular dynamics simulations. *J. Am. Chem. Soc.* 132:7549–7555.
25. Du, Z., Y. Liu, ..., C. Wang. 2010. Backbone dynamics and global effects of an activating mutation in minimized Mtu RecA inteins. *J. Mol. Biol.* 400:755–767.
26. Earnhardt, J. N., S. K. Wright, ..., D. N. Silverman. 1999. Introduction of histidine analogs leads to enhanced proton transfer in carbonic anhydrase V. *Arch. Biochem. Biophys.* 361:264–270.
27. Ellman, G. L. 1959. Tissue sulfhydryl groups. *Arch. Biochem. Biophys.* 82:70–77.
28. Kelemen, B. R., T. A. Klink, ..., R. T. Raines. 1999. Hypersensitive substrate for ribonucleases. *Nucleic Acids Res.* 27:3696–3701.
29. Park, C., B. R. Kelemen, ..., R. T. Raines. 2001. Fast, facile, hypersensitive assays for ribonucleolytic activity. *Methods Enzymol.* 341:81–94.
30. Loria, J. P., M. Rance, and A. G. Palmer. 1999. A relaxation-compensated Carr-Purcell-Meiboom-Gill sequence for characterizing chemical exchange by NMR spectroscopy. *J. Am. Chem. Soc.* 121:2331–2332.
31. Kovrigina, E. L., J. G. Kempf, ..., J. P. Loria. 2006. Faithful estimation of dynamics parameters from CPMG relaxation dispersion measurements. *J. Magn. Reson.* 180:93–104.
32. Wlodawer, A., L. A. Svensson, ..., G. L. Gilliland. 1988. Structure of phosphate-free ribonuclease A refined at 1.26 Å. *Biochemistry.* 27:2705–2717.
33. Case, D. A., T. E. Cheatham, 3rd, ..., R. J. Woods. 2005. The Amber biomolecular simulation programs. *J. Comput. Chem.* 26:1668–1688.
34. Phillips, J. C., R. Braun, ..., K. Schulten. 2005. Scalable molecular dynamics with NAMD. *J. Comput. Chem.* 26:1781–1802.
35. Wang, J., R. M. Wolf, ..., D. A. Case. 2004. Development and testing of a general amber force field. *J. Comput. Chem.* 25:1157–1174.
36. Bayly, C. I., P. Cieplak, ..., P. Kollman. 1993. A well-behaved electrostatic potential based method using charge restraints for deriving atomic charges - The RESP model. *J. Phys. Chem.* 97:10269–10280.
37. Frisch, M. J., G. W. Trucks, ..., D. J. Fox. 2009. Gaussian 09, Revision A.1. Gaussian, Wallingford, CT.
38. Jorgensen, W. L., J. Chandrasekhar, ..., M. Klein. 1983. Comparison of simple potential functions for simulating liquid water. *J. Chem. Phys.* 79:926–935.
39. Darden, T., D. York, and L. Pedersen. 1993. Particle mesh Ewald: an N-log(N) method for Ewald sums in large systems. *J. Chem. Phys.* 89:10089–10092.
40. Grubmüller, H., H. Heller, ..., K. Schulten. 1991. Generalized Verlet algorithm for efficient molecular dynamics simulations with long-range interactions. *Mol. Simul.* 6:121–142.
41. Ichiye, T., and M. Karplus. 1991. Collective motions in proteins: a covariance analysis of atomic fluctuations in molecular dynamics and normal mode simulations. *Proteins.* 11:205–217.
42. Weiner, H., W. N. White, ..., D. E. Koshland, Jr. 1966. The formation of anhydrochymotrypsin by removing the elements of water from the serine at the active site. *J. Am. Chem. Soc.* 88:3851–3859.
43. Neet, K. E., and D. E. Koshland, Jr. 1966. The conversion of serine at the active site of subtilisin to cysteine: a “chemical mutation”. *Proc. Natl. Acad. Sci. USA.* 56:1606–1611.
44. Polgar, L., and M. L. Bender. 1966. A new enzyme containing a synthetically formed active site. Thiol-subtilisin. *J. Am. Chem. Soc.* 88:3153–3154.
45. Smith, H. B., and F. C. Hartman. 1988. Restoration of activity to catalytically deficient mutants of ribulosebiphosphate carboxylase/oxygenase by aminoethylation. *J. Biol. Chem.* 263:4921–4925.
46. Gloss, L. M., and J. F. Kirsch. 1995. Decreasing the basicity of the active site base, Lys-258, of *Escherichia coli* aspartate aminotransferase by replacement with gamma-thialysine. *Biochemistry.* 34:3990–3998.
47. Gloss, L. M., and J. F. Kirsch. 1995. Examining the structural and chemical flexibility of the active site base, Lys-258, of *Escherichia coli* aspartate aminotransferase by replacement with unnatural amino acids. *Biochemistry.* 34:12323–12332.
48. Waldman, A. D., B. Birdsall, ..., J. J. Holbrook. 1986. 13C-NMR and transient kinetic studies on lactate dehydrogenase [Cys(13CN)165]. Direct measurement of a rate-limiting rearrangement in protein structure. *Biochim. Biophys. Acta.* 870:102–111.
49. Cellitti, S. E., D. H. Jones, ..., B. H. Geierstanger. 2008. In vivo incorporation of unnatural amino acids to probe structure, dynamics, and ligand binding in a large protein by nuclear magnetic resonance spectroscopy. *J. Am. Chem. Soc.* 130:9268–9281.

50. Cornish, V. W., D. R. Benson, ..., P. G. Schultz. 1994. Site-specific incorporation of biophysical probes into proteins. *Proc. Natl. Acad. Sci. USA.* 91:2910–2914.
51. Lampe, J. N., S. N. Floor, ..., P. R. Ortiz de Montellano. 2008. Ligand-induced conformational heterogeneity of cytochrome P450 CYP119 identified by 2D NMR spectroscopy with the unnatural amino acid (13)C-p-methoxyphenylalanine. *J. Am. Chem. Soc.* 130:16168–16169.
52. Miyake-Stoner, S. J., C. A. Refakis, ..., R. A. Mehl. 2010. Generating permissive site-specific unnatural aminoacyl-tRNA synthetases. *Biochemistry.* 49:1667–1677.
53. Weeks, C. L., A. Polishchuk, ..., T. G. Spiro. 2008. Investigation of an unnatural amino acid for use as a resonance Raman probe: detection limits, solvent and temperature dependence of the nuC identical withN band of 4-cyanophenylalanine. *J Raman Spectrosc.* 39:1606–1613.
54. Zheng, M. L., D. C. Zheng, and J. Wang. 2010. Non-native side chain IR probe in peptides: ab initio computation and 1D and 2D IR spectral simulation. *J. Phys. Chem. B.* 114:2327–2336.
55. Palmer, A. G., C. D. Kroenke, and J. P. Loria. 2001. Nuclear magnetic resonance methods for quantifying microsecond-to-millisecond motions in biological macromolecules. *Meth. Enzymol.* 339:204–238.
56. Doucet, N., G. Khirich, ..., J. P. Loria. 2011. Alteration of hydrogen bonding in the vicinity of histidine 48 disrupts millisecond motions in RNase A. *Biochemistry.* 50:1723–1730.
57. Cathou, R. E., and G. G. Hammes. 1964. Relaxation spectra of ribonuclease. I. The interaction of ribonuclease with cytidine 3'-phosphate. *J. Am. Chem. Soc.* 86:3240–3245.
58. Cathou, R. E., and G. G. Hammes. 1965. Relaxation spectra of ribonuclease. 3. Further investigation of the interaction of ribonuclease and cytidine 3'-phosphate. *J. Am. Chem. Soc.* 87:4674–4680.
59. Park, C., and R. T. Raines. 2001. Quantitative analysis of the effect of salt concentration on enzymatic catalysis. *J. Am. Chem. Soc.* 123: 11472–11479.
60. Rutkoski, T. J., and R. T. Raines. 2008. Evasion of ribonuclease inhibitor as a determinant of ribonuclease cytotoxicity. *Curr. Pharm. Biotechnol.* 9:185–189.